Directional spectrum of wind-generated ocean waves

By MAHINDER S. UBEROI
Department of Aerospace Engineering Sciences and the
Joint Institute for Laboratory Astrophysics, University of Colorado, Boulder,
and Department of Aeronautical and Astronautical Engineering,
University of Michigan, Ann Arbor, Michigan

(Received 6 September 1963)

Two sets of published data on an area 2700 ft. by 1800 ft. of sea surface in the North Atlantic are analysed by an optical computer which gives directly the directional spectrum. The results are compared with (i) those of other investigators obtained laboriously by using a digital computer, (ii) the frequency spectrum, and (iii) an empirical prediction.

1. Introduction

Consider a single gravity wave in a direction making an angle θ with the x_1-axis on an unbounded ocean. According to the linearized equation of motion and for infinite ocean depth, the wave height

$$h(x_1, x_2 t) \sim \exp\{i(k_1x_1+k_2x_2-\omega t)\} \tag{1}$$

where the wave-number $k = (k_1^2+k_2^2)^{\frac{1}{2}}$, $\theta = \tan^{-1}(k_2/k_1)$, $\omega^2 = kg$ and g is the gravitational acceleration. Now consider a large ocean surface over which steady wind has been blowing for long enough time to produce statistically steady and homogeneous waves. We define a correlation

$$R(y_1, y_2, \tau) = \lim_{\substack{L\to\infty \\ T\to\infty}} (8L^2T)^{-1}\int_{-T}^{T} dt \int_{-L}^{L} dx_1 \int_{-L}^{L} dx_2\, h(x_1, x_2, t)\, h(x_1+y_1, x_2+y_2, t+\tau). \tag{2}$$

It can be shown that

$$R(y_1, y_2, \tau) = \int_{-\infty}^{\infty} dk_2 \int_0^{\infty} dk_1 E(k_1, k_2)\cos(k_1y_1+k_2y_2-\omega\tau), \tag{3}$$

and in particular

$$R(y_1, y_2, 0) = \int_{-\infty}^{\infty} dk_2 \int_0^{\infty} dk_1 E(k_1, k_2)\cos(k_1y_1+k_2y_2), \tag{4}$$

and
$$R(0,0,\tau) = \int_0^{\infty}\left[g^{-\frac{1}{2}}\int_0^{\pi} k^{\frac{3}{2}}E(k,\theta)\,d\theta\right]\cos\omega\tau\,d\omega, \tag{5}$$

where
$$F(\omega) = g^{-\frac{1}{2}}\int_0^{\pi} k^{\frac{3}{2}}E(k,\theta)\,d\theta. \tag{6}$$

The directional spectrum E is also given by the relation

$$E(k_1, k_2) = \lim_{L\to\infty} (4L\pi)^{-2}\left|\int_{-L}^{L}\int_{-L}^{L} h(x_1, x_2, t)\exp\{i(k_1x_1+k_2x_2)\}\,dx_1dx_1\right|^2 \tag{7}$$

and can be directly determined from the instantaneous surface height of a sufficiently large sea. The frequency spectrum $F(\omega)$ is also given by the relation

$$F(\omega) = \lim_{T\to\infty} (4T\pi)^{-1} \left| \int_{-T}^{T} h(x_1, x_2, t)\, e^{i\omega t} dt \right|^2 \tag{8}$$

and may be determined from surface height measured at one point using a wave-pole and is sometimes called wave-pole spectrum. For large but finite L and T,

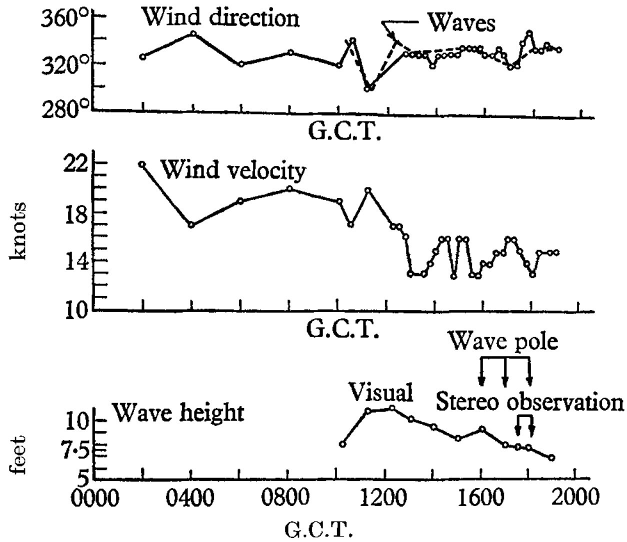

FIGURE 2. The wind and sea conditions during and prior to the observations (from SWOP).

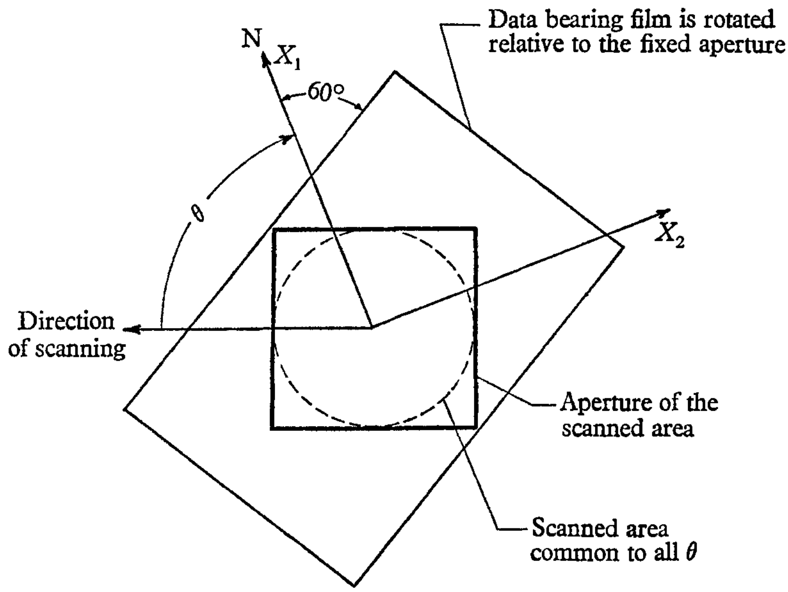

FIGURE 3. The position of the scanned area relative to the data bearing film.

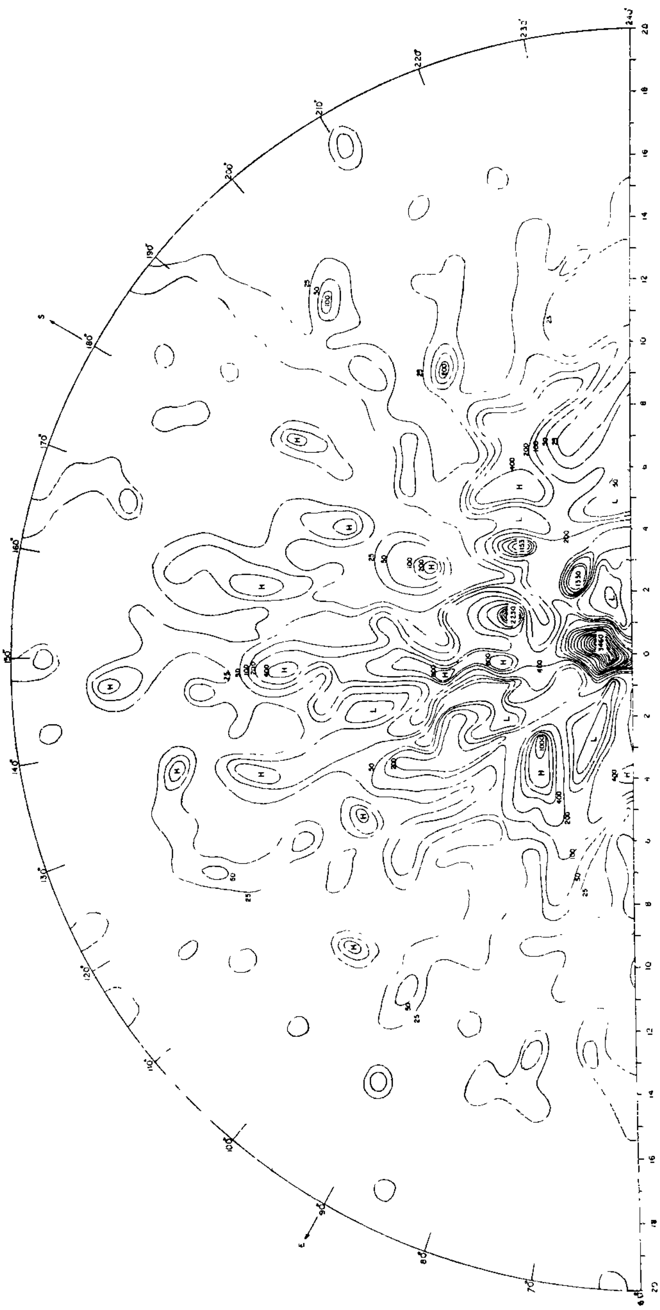

FIGURE 4. Normalized directional spectrum

$$E(k, \theta) \Big/ \left\{ \int_0^{31\cdot 5} dk \int_0^{\pi} d\theta E(k, \theta) \right\}.$$

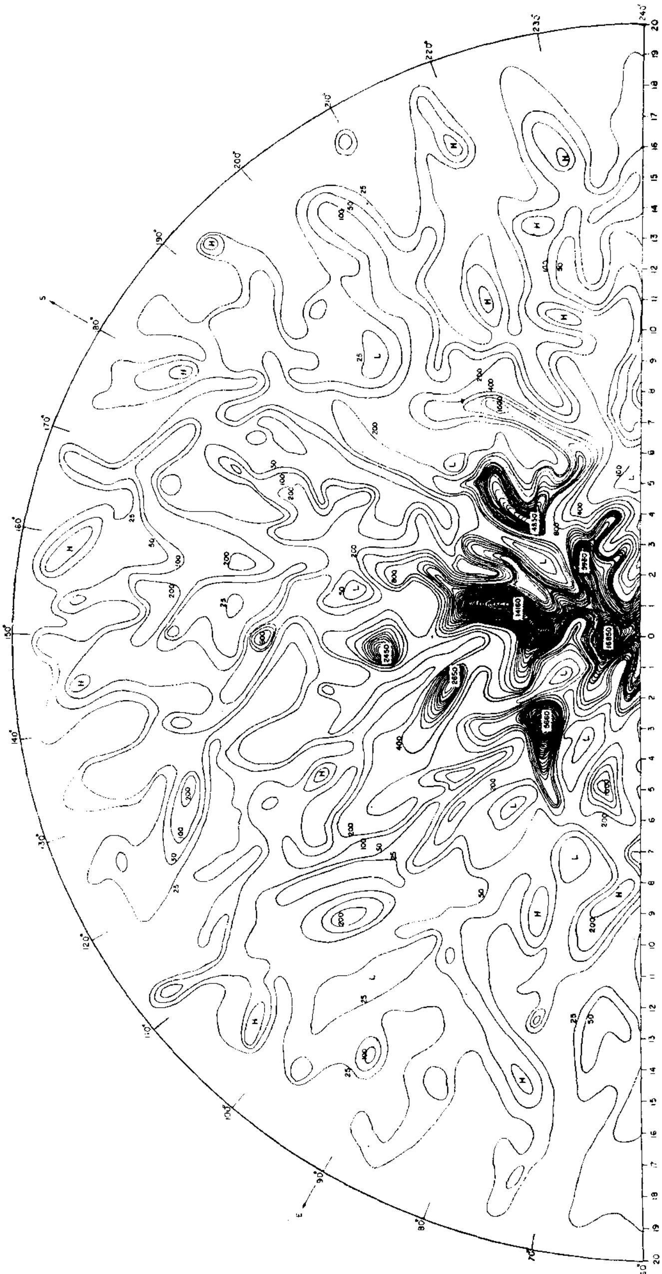

FIGURE 5. Normalized directional spectrum

$$E(k,\theta)\Big/\left\{\int_0^{31\cdot5} dk \int_0^{\pi} d\theta\, E(k,\theta)\right\}$$

for the data set 3.

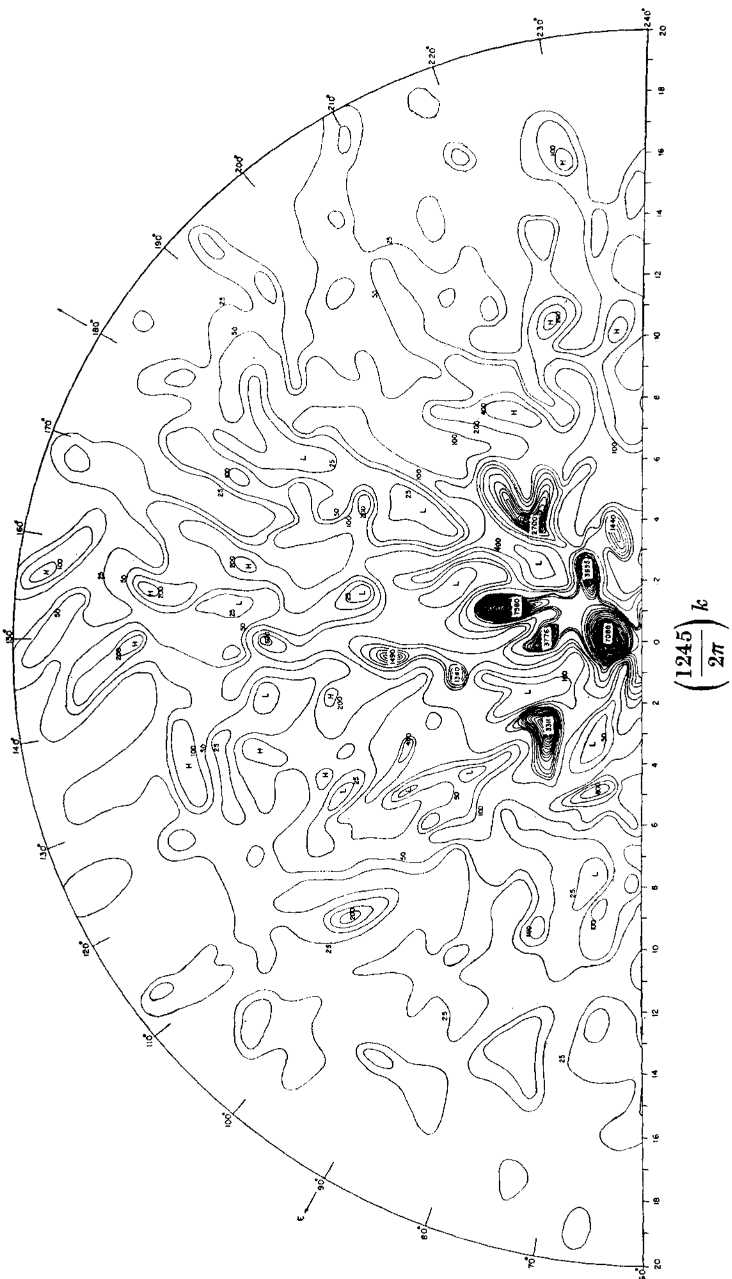

FIGURE 6. Average of normalized spectra for the data sets 2 and 3.

the equations (3), (7) and (8) follow from elementary properties of Fourier transform and for $L \to \infty, T \to \infty$, we assume that the limits exist (see, for example, Pierson 1955). The directional spectrum gives complete spectral information about the waves and the wave-pole spectrum may be determined from it while the reverse is not true.

2. Observations of sea-surface roughness

Simultaneous stereo-photographs were taken on 25 October 1954, by two aeroplanes flying in tandem over the North Atlantic at latitude 39 N. and longitude 63·5 W. as a part of the Stereo Wave Observation Project (SWOP 1956). Instantaneous heights were determined by SWOP from two sets of

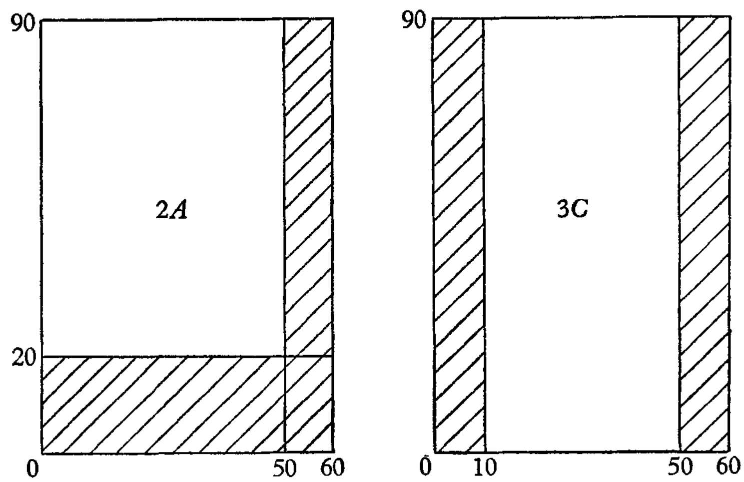

FIGURE 7. Schematic representation of the subset 2*A* and 3*C* for the sets 2 and 3 used by SWOP to calculate the directional spectra.

stereo-photographs at discrete points 30 ft. apart covering an area 2700 ft. by 1800 ft., and are given in the SWOP report (1956). The accuracy of the heights is $\pm 0{\cdot}5$ ft. and that of the horizontal location of the points is ± 2 ft. We have transcribed each set of 90×60 points onto a photographic film such that its transparency at each point is proportional to local wave height as shown in plate 1, figure 1. In actual practice the sea surface height was quantized in levels 0·5 ft. apart. Maximum variations in sea surface height is from $-9{\cdot}5$ ft. to $+9{\cdot}5$ ft. giving 38 quantized levels. 0·30 in. square holes were punched in an 18 in. by 27 in. black paper at points corresponding to locations on the sea surface which have the same quantized level. In a similar manner, a mask was prepared for each quantized level. Each mask was placed over a uniformly bright surface 18 in. by 27 in., and a picture of the combination taken on the same photographic film. From the known calibration of the film the time of exposure for each mask was adjusted so that for each square the transparency of the film is proportional to the corresponding sea-surface height. The film used was Kodak Panatomic X developed in D 76 for 18 min. at 69 °F.

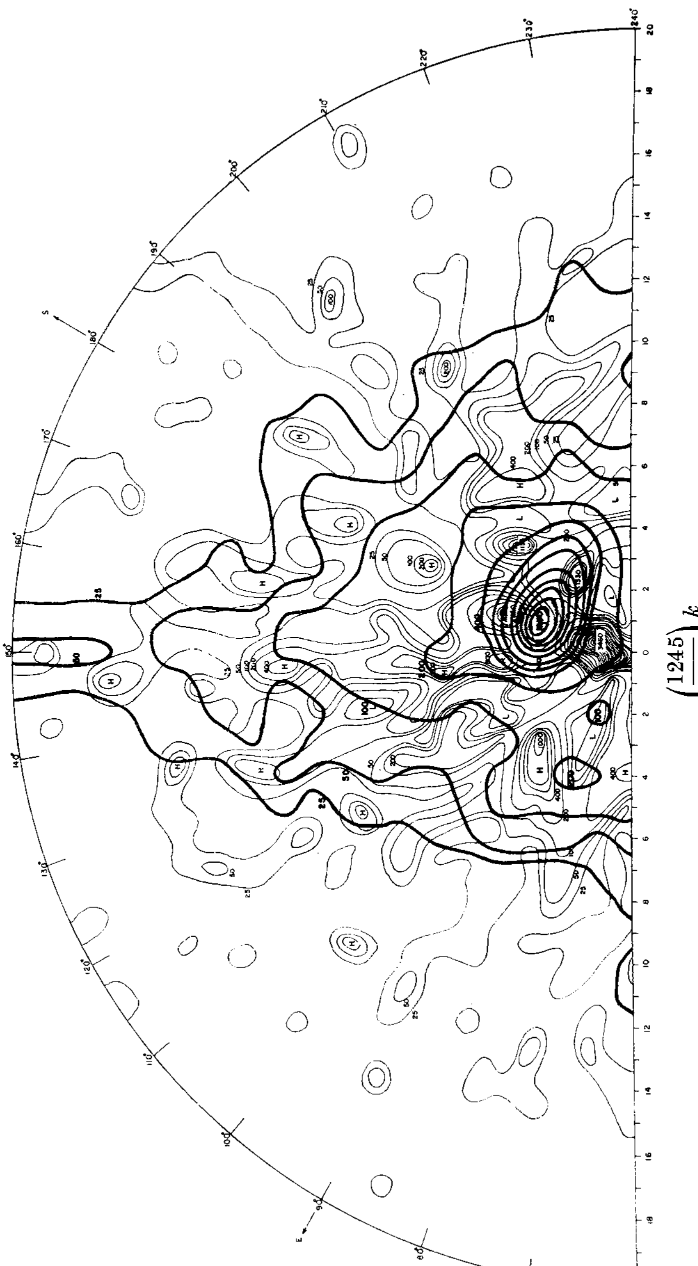

FIGURE 8. Comparison of normalized direction spectra

$$E(k,\theta)\Big/\left\{\int_0^{31\cdot 5} dk \int_0^{\pi} d\theta E(k,\theta)\right\}$$

for data set 2 with that computed by SWOP for data set 2*A* and represented here by heavy lines.

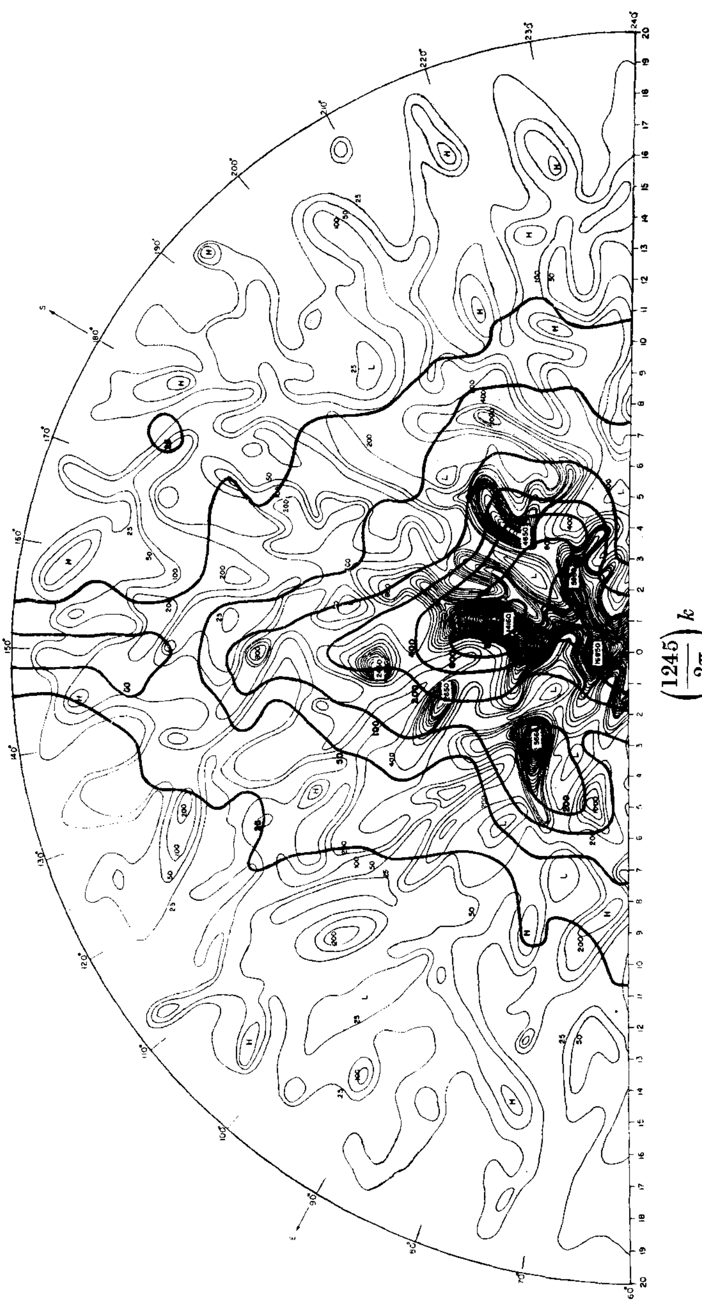

FIGURE 9. Comparison of normalized direction spectra

$$E(k,\theta)\Big/\left\{\int_0^{\pi/31\cdot 5} dk \int_0^{\pi} d\theta E(k,\theta)\right\}$$

for data set 3 with that computed by SWOP for data set 3C and represented here by heavy lines.

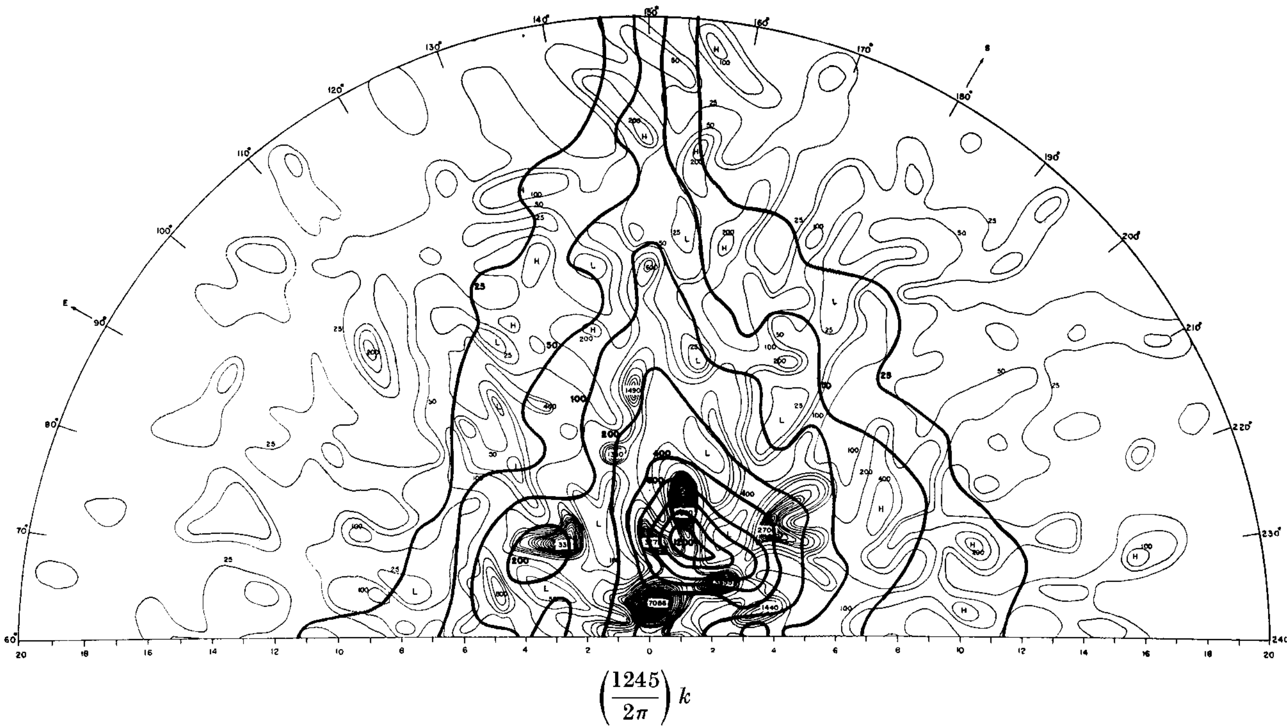

FIGURE 10. Comparison of the average of spectra for data sets 2 and 3 with the corresponding SWOP results.

The wave height as a function of time was determined by an oceanographic research vessel stationed in the same area using a wave-pole. The frequency spectrum of the waves was found in this way, and will be referred to later. The wind and the sea conditions during and prior to these observations are shown in figure 2.

3. Directional spectra

$E(k, \theta)$ was determined for the two sets by scanning the data bearing film with a long and narrow beam of light and the transmitted light was measured with a photocell whose output was passed through a narrow pass band filter corresponding to a fixed wave-number k. The mean-square output of the filter is proportional to E for a fixed k and θ (for the details, see Uberoi 1962). The scanned area corresponds to a square aperture covering 41·5 by 41·5 data points as shown in figure 3. The dependence of E on θ is obtained by rotating the film relative to the fixed aperture. The dependence of E on k is obtained by changing the pass band of the filter. Since the scanned area corresponds to $(41{\cdot}5 \times 30)$ ft. by $(41{\cdot}5 \times 30)$ ft. of the sea surface area the minimum wave-number is $(2\pi/41{\cdot}5 \times 30)\,\text{ft.}^{-1}$. The maximum wave-number, which is roughly limited by the quantization of the data, was chosen to be 20 times the minimum. The contour maps of the normalized spectra are shown in figures 4 to 6. The mean square heights for the entire sets 2 and 3 are 4·61 and 4·30 ft.^{2} respectively. Although the scanned area does not cover the entire set the quantity

$$\int_0^{\pi/31\cdot 5} dk \int_0^{\pi} d\theta E(k, \theta)$$

for each data set is very close to the mean square height for the entire set. The general nature of the two spectra are the same. The high values of E for set 2 are approximately three times the corresponding values for set 3, which probably is due to statistical fluctuations. However, these peaks contribute relatively little to the total energy.

The same data were originally analysed on a digital computer as described in the SWOP report. The auto-correlation was first computed and then smoothed; the Fourier transform of the latter gave E. When the entire data of each set were used, the computed E's were negative for some wave-number which is the result either of errors in numerical calculations or of the assumptions used in obtaining the estimated auto-correlation being such that it is not positive definite. For this and other reasons, portions of the two sets of data as shown in figure 7 were used. The computed E's were smoothed by using a two-dimensional filter and the normalized spectra are compared with the present analysis in figures 8 to 10. In the SWOP calculations

$$k = \frac{2\pi n}{1200}\,\text{ft.}^{-1} \quad (n = 0, 1, \ldots, 20),$$

and the normalization factor is

$$\int_0^{\pi/30} dk \int_0^{\pi} d\theta\, E(k, \theta),$$

while in our case

$$k = \frac{2\pi n}{1245}\,\text{ft.}^{-1} \quad (n = 0, 1, \ldots, 20),$$

and the normalization factor is

$$\int_0^{\pi/31\cdot5} dk \int_0^{\pi} d\theta\, E(k,\theta).$$

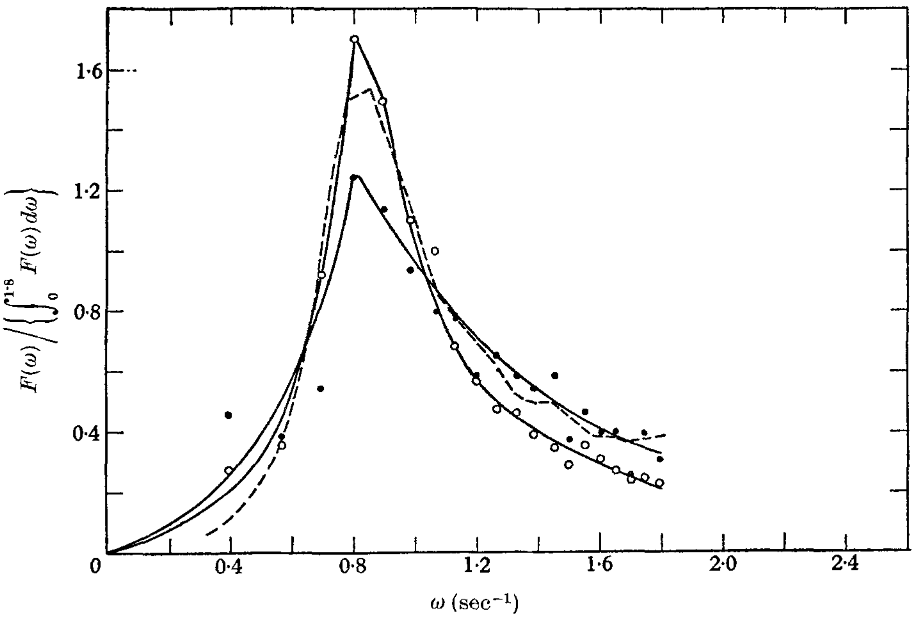

FIGURE 11. Comparison among the frequency spectra

$$F(\omega)\Big/\left\{\int_0^{1\cdot8} F(\omega)\,d\omega\right\}$$

computed from the directional spectra. ○, Data set 2; ●, data set 3; ----, SWOP calculations based on the average of sets $2A$ and $3C$.

These small differences are neglected here. Our method gives E as a function of k and θ and the spectrum is determined for many more points near zero wave-number than SWOP calculation which gives E as a function of k_1 and k_2. This is an advantage in determining any direction spectra. We find a distinct peak in the values of E near the origin for both sets while the SWOP calculations show a high value in the same region but no distinct peak. While the SWOP analysis shows one main high peak our data show several peak in the same area. Some of the smaller peaks might disappear if the E's were smoothed as by SWOP but major peaks would still remain. Our analysis shows that the high values of E for set 2 are approximately three times the corresponding values for set 3 while the reverse is the case for the SWOP calculation for data sets $2A$ and $3C$.

4. Comparison with wave-pole and theoretical spectra

The wave-pole data has been analysed by SWOP to determine the frequency spectrum. The mean square heights based on the entire sets of stereo data are

4·61 and 4·30 ft.^{2} for sets 2 and 3 and 2·49 ft.^{2} for the wave-pole data. SWOP has applied various corrections, such as white noise, to the spectra to bring the results close together. These corrections are involved and some of them appear to be of doubtful value. Here we consider the normalized frequency spectrum

$$F(\omega)\Big/\left\{\int_0^{1\cdot 8} F(\omega)\,d\omega\right\}$$

determined by various means. When normalizing we integrate the spectrum from $\omega = 0$ to 1·8 sec.$^{-1}$ which corresponds to the upper-wave-number $(\pi/31\cdot 5)$ for the directional spectrum.

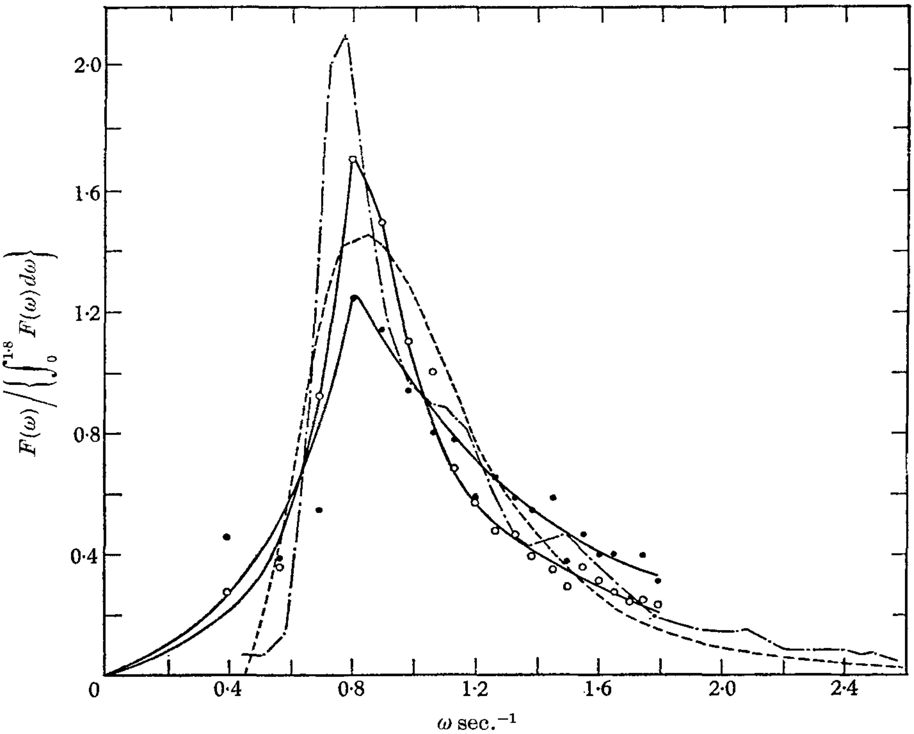

FIGURE 12. Comparison among the frequency spectra

$$F(\omega)\Big/\left\{\int_0^{1\cdot 8} F(\omega)\,d\omega\right\}:$$

○ (set 2) and ● (set 3) from the directional spectra; —·—, from the wave-pole data; ----, Neumann spectrum for 18·5 knots.

In our case E is known as a function of θ and the frequency spectrum may be easily computed from the directional spectrum. SWOP has also calculated the wave-pole spectrum from their average directional spectrum. These results are compared with those obtained by SWOP in figure 11. The average of the two spectra is quite close to the SWOP computation. In figure 12, the frequency spectra computed from the directional spectra are compared with the measured wave-pole spectrum and the empirical spectrum (Neumann 1954) for wind speed of 18·5 knots.

5. Sources of error

The calibration of the film and the stability of the photocell are accurate to within $\pm 2\%$. The little bands of white that border the squares in the figures 1 (*a*) and 1 (*b*) are due to imperfections in the masks for the quantized heights. The sharp bands have a very wide spectrum of the nature of isotropic white noise and have little effect on the directional properties of the measured spectrum. The relative area of these bands is small and hence their contribution to the spectrum is also small. The scanning slit has a width of 0·01 in. and smooths out some of these bands which are approximately of the same width.

This work was supported by The Fluid Dynamics Division of the Office of Naval Research under Contract Nonr 1224(02). The assistance of Messrs Stanley Wallis and Stuart Bowen is gratefully acknowledged.

REFERENCES

NEUMANN, G. 1954 Zur Charakteristik des Seeganges. *Archiv. Meteorol. Geophysik und Bioklimat*, A, **7**, 352.

PIERSON, W. J. 1955 *Advances in Geophysics*, vol. 2. New York: Academic Press Inc.

SWOP 1956 The directional spectrum of a wind generated sea as determined from the data obtained by stereo wave observation project. *Engineering College, New York University.*

UBEROI, M. S. 1962 *Rev. Sci. Inst.* **33**, 314.